SIN-CHN SCIENTIFIC PRESS PTE.LTD.

Molecular & Cellular Biomechanics 2024, 21(4), 371.
https://doi.org/10.62617/mcb371

Article

Biomechanics based computer simulation of rural landscape design using remote sensing image technology

Kun Xing[1,2], Yuqing Xia[3,*]

[1] Academy of Art and Design, Anhui University of Technology, Ma'anshan 243032, Anhui, China
[2] key Laboratory of Multidisciplinary Management and Control of Complex Systems of Anhui Higher Education Institutes Anhui University of Technology, Ma'anshan 243032, Anhui, China
[3] Academy of Art and Design, Anhui University of Technology, Ma'anshan 243032, Anhui, China
*** Corresponding author:** Yuqing Xia, 13955599088@163.com

CITATION

Xing K, Xia Y. Biomechanics based computer simulation of rural landscape design using remote sensing image technology. Molecular & Cellular Biomechanics. 2024; 21(4): 371. https://doi.org/10.62617/mcb371

ARTICLE INFO

Received: 14 September 2024
Accepted: 30 September 2024
Available online: 30 December 2024

Abstract: Introduction: The strategy and restoration of rural areas and landscape in biomechanics, with a particular emphasis on cellular and molecular biomechanics, is crucial for sustainable rural landscape design. At the cellular and molecular level, plants' biomechanical properties, such as the rigidity and elasticity of cell walls, determine their growth patterns and responses to environmental factors. These properties are essential in understanding how plants can be effectively incorporated into the rural landscape to enhance its stability and functionality. Aim: The objective of this research is to develop a novel computer simulation model for rural landscape planning using remote sensing imaging technology. Research methodology: We introduce a novel Adaptive YOLOv7 method driven by Starling Murmuration search. UAVs are used to collect extensive visual data for training the model. By considering cellular and molecular biomechanics, we can analyze how the mechanical forces within plants affect their ability to resist wind, retain water, and interact with the surrounding soil and other organisms. This knowledge can be integrated into the model to better predict the long-term viability and adaptability of different plant species in the rural landscape. The combination of the 3D GIS virtual image strategy model and our proposed model, along with SM optimization, not only improves object identification but also takes into account the biomechanical aspects for more accurate simulations. Crowdsourcing helps in precisely mapping rural landscapes and structures, while the incorporation of biomechanical principles ensures better adaptability to changing environmental and ecological conditions. Findings and Conclusion: Implemented in Python software, our SM-AYOLOv7 model shows excellent performance, with metrics like f1 score (93.64%), recall (92.34%), accuracy (91.72%), and IoU (90.23%). Our method outperforms conventional ones, demonstrating enhanced accuracy and flexibility, especially in handling changing configurations, due to the integration of cellular and molecular biomechanical insights.

Keywords: rural landscape design; remote sensing; image processing; starling murmuration search-driven adaptive YOLOv7 (SM-AYOLOv7); computer simulation; plant biomechanical properties

1. Introduction

Rural photography is the hub where environmental sustainability, cultural conservation and community welfare come together. It is a complete philosophy of conservation that unites natural elements with human activities through which biodiversity [1] sustainability and identity of people's culture are conserved. The folk dwellings historically dependent on the ecosystem as a source of livelihood and

a habitat will maintain ecological balance through a professional and thorough design of the open spaces which will result in meeting the development needs of the community in the future [2]. Landscaping rural landscape designs, through the utilization of native plants in gardens, shaping the natural landscape forms and management of the water resources, strive to generate productive and appealing gardens. Likewise, native plants or plant life not only keep the integrity of the system but also provide food and shelter for the wildlife in the region [3].

Erosion-reduction techniques that include terrace and contouring of the land are the role of landform manipulations [4]. Climate diversification is another factor that impacts land manipulation [5]. The implementation of management strategies of water such as rainwater harvesting and wetland restoration is important in reinstating ecosystems and conserving limited water resources, too [6]. Furthermore, beyond safeguarding the natural habitats, the rural landscaping looks into the human welfare as well as the culture of people. This is two-pronged with mindful planning and stewardship being vital in the procedure to make sure that all development-related activities are properly done in giving the ecosystems due to respect [7].

The rural landscape design grabs sustainability and preserves biodiversity but also creates a livelihood for the local people [8]. In the present time, these developments in the technology of remote sensing images have transitioned the landscape design using knowledge, analysis and visualization tools [9]. Remotely sensing technology using satellite imaging, aerial shots, and drone data will bring in the quality needed by designers to make informed decisions about land use, habitats and urban development using biomechanics [10].

To develop and validate an innovative computer simulation model for design of rural landscapes with remote sensing image devices, combining the SM-AYOLOv7 algorithm for precise classification.

Key Contributions:

- The SM-AYOLOv7 algorithm of rural buildings and rural environments identification through remote sensing images is introduced, thus, the classification accuracy is improved.
- When rural landscape designs are simulated using 3D GIS virtual image design models, thus helping to visualize and plan for the rural landscape design.
- The proof of the superior performance of the new techniques over the traditional methods is the increase in accuracy and adaptability in dynamic situations.

Section II: Surveys relevant studies on landscape design and remote sensing. Section III: Describes the Research area (Lingxi Valley). Section IV: Introduces SM-AYOLOv7 algorithm and research approach. Section V: Presents experimental findings and comparisons. Section VI: Summarizes outcomes and suggests future research.

2. Literature review

By contrasting the outdoor and indoor designs, the author of [11] explored the use and optimization of virtual reality (VR) technology in landscape design. It attempted the integration of VR and VR-GIS, as well as traditional for energy

savings. An effective technique for VR landscape design, the Lumia VR platform was utilized for auxiliary usage and detail optimization. Its consistent visual modeling inaccuracy and 8.9-second rendering time were noteworthy features.

Study on 3D visualized urban landscape design and planning was covered in the paper [12] with particular attention paid to the historical context of the field, present difficulties and the fundamentals of the spatial roaming sorting method. Along with conducted simulation tests, it covered the integration and optimization of landscape design concepts. The outcomes demonstrated by offered realistic data processing effects, virtual reality technology-enhanced design quality and efficiency.

Using a 3D city GIS study [13] investigated to create a virtual city. The basics of city 3D simulation were covered, along with the process of created a 3D city environment and its evolution through biomechanics. The research examined the relevance and future of dynamic simulation technologies in urban 3D environments. To assure progress and dependability, the study put out a thorough assessment metric system based on visual components and sensibility.

A novel method for simulated garden landscape distributed logic using VR and 3D images was provided in the research [14]. It suggested a technique for employed camera posture matrices and Speeded-Up Robust Features (SURF) feature point recognition to analyze landscape garden distribution logically. Results from performance tests and case analyses were utilized to show the excellence of the technology, which was subsequently used for research and rebuilding.

Research utilizing excellent quality remote sensing photos to create a model for the distribution of species was published in paper [15]. The model operates better than traditional models and collects data on the landscape and ecosystem at precise scales of space. Using t-distributed Stochastic Neighbour Embedding (t-SNE) reduction of dimensions, which visualizes input data and environmental variance, the ecological importance of the framework was illustrated.

By applying the highest probability classification technique, urban buildings were found in the research [16] employed local climate zones. ENVI-met validated the effects of heat stress on urban structures by simulated microclimate in six idealized models. The data revealed a significant effect of different urban building styles on heat exhaustion, a regional variance in microclimate, and an accuracy of 0.802.

An agent model was created, temporal granularity in simulation machine learning was discussed, and the agent model’s timeliness was investigated [17]. It investigated strategies for real-time assurance, real-time simulation and message interactivity. Additionally, the article offered comparisons between AutoCAD and conventional design methods, and biomechanics that are highlighted the sophisticated, scientific and rational nature of machine learning.

The influence of satellite imagery for the greening of cities on residential landscape design was studied by the author of [18]. The SURF color remote sensing image analysis technique and a greening remote sensing image processed algorithm were employed. According to the study, urban gardens may maximize building utilization while offered amusement and lowering people’s stress levels. Results indicated a 94% accuracy rate in recognized green building characteristics.

Using wireless sensor networks and neural networks, the research [19]

investigated intelligent landscape design and land planning using biomechanics. Urban landscape planning was greatly affected by parametric designing, which affected construction and design as well. The utilization of urban land was enhanced, waste was decreased, and resource efficiency was increased with the use of digital design for landscaping.

Land production, lifestyle and natural spaces were the main topics of [20]'s study, which examined spatial equitable growth in the Poyang Lake area. Four scenarios of changes in 2030 were simulated using the random forest Markov future land use simulation (RF-Markov-FLUS) coupled model: integrated development (ID). The findings implied that better urban planned efficiency, established communities and agricultural production should be the main goals of geographic pattern optimization.

With an emphasized on smart intercommunication systems for landscaping, water conservation and environmental protection the author of [21] talked about the creation of a smart city management framework. The IoT, building data modeling, integrated digital systems, and geographic data modeling were utilized by the framework. The research established its usefulness in governance by using the data platform to acquire, transmit, analyze and process data.

By utilizing cutting-edge geospatial and machine learning tools, the study [22] evaluated the vulnerabilities, of a wetland environment in Pakistan. In terms of classifying land cover, the random forest approach produced the best results (89.5%), indicating an 11% decrease in open water bodies. The study offered useful conservation planning insights as well as a baseline for long-term management and protection of wetlands.

To identify and distinguish glass greenhouses and mulching films from excellent quality remotely sensed data, a deep learning model was presented in the work [23]. The model was made up of a dilatation and non-local convolutional neural network (DNCNN) that aggregates spatial data while extracted global and contextual factors. The results of the study indicated high accuracy of 89.6% and 92.6%, with convolution dilated enhanced an accuracy rate of 2.7% and non-local extracted features improved accuracy around 2%.

Using remote sensing technologies, the study of [24] suggested a way of the spatiotemporal evolution of urban complicated landscape structures. The strategy lowered dry land area, decreased residential, industrial and mining land transfer volume and improved stability. Urban fragmentation was becoming more profound as seen by the growing density of landscape borders. Total design alignment demonstrated the method's strong application efficacy.

To examine past and future land use/cover changes (FLUCCs), [25] conducted a study using remote sensing data. The findings indicated a considerable loss of agricultural land and vegetation together with the rapid development of urban building areas. The only sort of land usage that significantly decreased in future models was agriculture. The largest growth in building land was in metropolitan areas between 2020 and 2030, mostly due to population migration and increasing urbanization.

3. Research area

Situated roughly between 118°17′30″ E–118°23′10″ E and 27°30′20″ N–27°25′15″ N, Lingxi Valley is found in the north eastern region of Fujian Province, China. Lingxi Valley covers 35.4 square km and is home to eight official communities as well as 30 unincorporated settlements. Situated in the southern portion of the valley, the major administrative settlement is a combination of flatlands and undulating hills with a network of waterways. The core administrative hamlet is about 5 km east of Qingzhou's principal town and around 40 km from the heart of Ningde City. The principal administrative village is flanked on the south and west by other noteworthy administrative communities. 30 natural settlements are spread across the valley and face problems such as steep inclines, poor infrastructure, twisting and narrow roads, and restricted access to modern services. Lingxi Valley's population was 3100 people and 1450 houses at the end of 2021. The economy is composed mostly of ecotourism and mixed farming, with 2800 hectares of protected forest areas and 150 hectares of arable land. The province of Fujian's map is shown in **Figure 1**.

Figure 1. Map of Fujian province, China.

4. Methodology

WEBGIS technology, biomechanics and oblique photography were used to create a 3D GIS real-space digital town model for the pilot community, enabling cloud sharing and offline discussions. Building this 3D model with WEBGL (Web Graphics library) entailed data collection components. The component involved UAV 3D mapping (refer to **Figure 2**), employing the DJI Mavic 2 Pro UAV model

alongside ground DGPS (Differential Global Positioning System) for aerial image capture. The data acquisition process took place under ideal conditions, characterized by sunny, cloudless weather conditions and high air visibility. Oblique photographs, meticulously selected and organized, were imported into Agi soft Meta shape software to generate mesh point cloud models in LAS (Lidar LASer) format. Subsequently, WEBGL technology has been used to create an online platform for real-time spatial visualization.

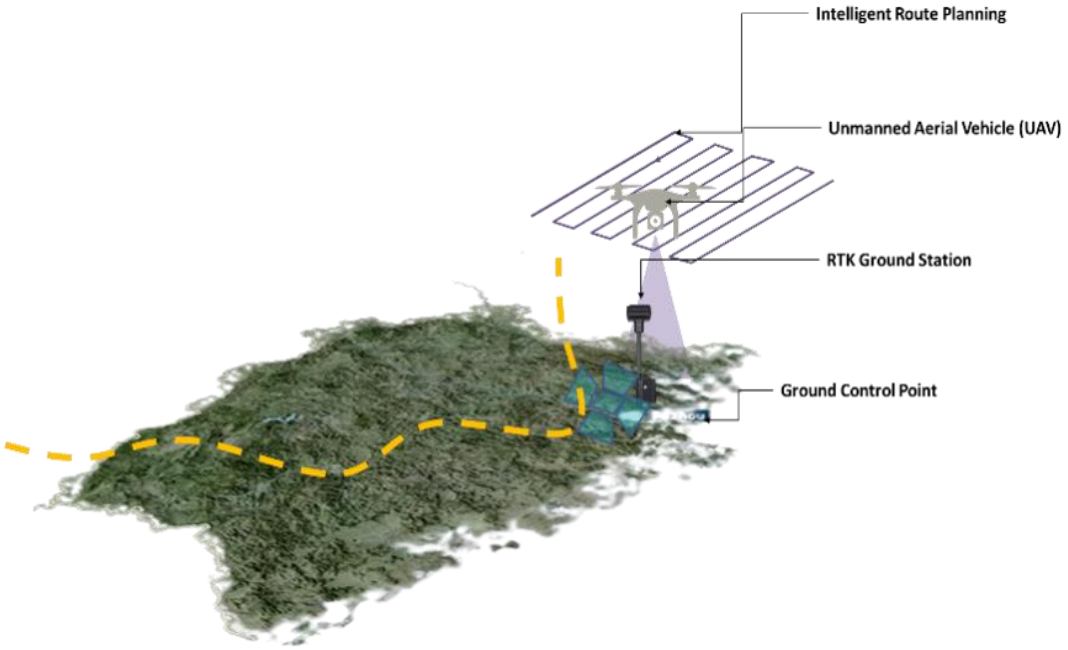

Figure 2. UAV 3D map.

Identifying and classifying various buildings

SM: The SM method simulates the behavior of starlings through their magnificent murmuration by employing three novel search methods: separating, diving, and spinning. The group of starlings is represented by the notation $T = \{t_1, t_2, \ldots, t_M\}$, where M is the group size. A value of a vector, $W_j(s) = (w_{j,1}, w_{j,2}, \ldots, w_{j,C})$, is used to indicate each starling t_j's location at iteration s. Its fitness score is indicated by $E_j(s)$. Equation (1) is used to start each $W_j(s)$ in the initial phase. The area of search is C-dimensional, with W^K and W^V representing the lower and upper limits, respectively, and $rand$ (0,1) representing a random number between 0 and 1.

$$W_j(s) = W^K + rand(1,0) \times (W^K - W^V), j = 1,2, \ldots, M \quad (1)$$

Employing the segregating, diving and swirling search tactics, the total number of starlings is shifted for the remaining iterations molecule. The next sections go into depth about each of these search techniques.

Separating Search Strategies: Diversity in society is encouraged by the separate search approach. Applying Equation (2), a part of starling's size O_{sep} are chosen at random from group T. Equation (3) is used to modify some of the chosen starlings' parameters. In this equation, $W_H(s)$ represents the entire best location, and $W_q(s)$ is

a selected starling from group T. At the end of each iteration, a random selection is made from these sets, and the best location thus far is saved. These locations are merged with the segregated locations of size O_{sep}. Applying Equation (4), one may derive the separation operator $R_1(z)$, where α represents the quantum harmonic oscillator, n, and l denote the mass and strength of the particle, and g represents a Planck constant. Additionally, the Hermite polynomial function G_m is associated with an int index m, whereas z is an arbitrary number.

$$O_{sep} = \frac{\log(s + C)}{\lg(MaxIt) \times 2} \tag{2}$$

$$W_j(s+1) = W_H(s) + R_1(z) \times \left(W_{q'}(s) - W_q(s)\right) \tag{3}$$

$$R_1(z) = \left(\frac{\alpha}{2^m \times m! \times \pi^{\frac{1}{2}}}\right)^{\frac{1}{2}} G_m(\alpha \times z) \times f^{-0.5 \times \alpha^2 \times z^2}, \alpha = \left(\frac{n \times l}{g}\right)^{\frac{1}{4}} \tag{4}$$

Either fluid multi-flock building, the remaining starlings having a size of $\acute{M}(M - O_{sep})$ are collected and used to search the issue space with swirling or diving search techniques. L non-empty flocks $(e_1, \ldots, e_l)$ are used in every cycle to form a changing multi-flock. The top l starlings are eliminated from group $\acute{M}$ and kept in matrix Q. The other population $(\acute{M} - Q)$ is dispersed between the l flocks. In the end, every flock is assigned a location in Q that is: $e_1 \leftarrow \{Q_1\ V\ e_l\}, \ldots e_l \leftarrow \{Q_l\ V\ e_l\}$.The condition of each flock determines which search methods, such as diving and spinning, are allocated to it, as Equation (6) illustrates. Equation (5) is used to determine each flock's effectiveness $\left(R_r(s)\right)$, where n is the aggregate number of starlings in every flock, l is the count of flocks, and $te_{ji}(s)$ is the starling's efficiency score in the flock e_i. Equation (6) uses the variable $\mu_R\ (s)$ to represent the average efficiency of all flock members.

$$R_r(s) = \frac{\sum_{j=1}^{l} \frac{1}{m} \sum_{i=1}^{m} te_{ji}(s)}{\frac{1}{m} \sum_{i=1}^{m} te_{ji}(s)} \tag{5}$$

$$W_j(s+1) = \begin{cases} \text{Diving search strategy} R_r(s) \le \mu_R(s) \\ \text{Whirling search strategy} R_r(s) > \mu_R(s) \end{cases} \tag{6}$$

Diving Search Strategy: To explore the area of search, the chosen flocks $\left(R_r(s) \le \mu_R(s)\right)$ are urged to use the diving search technique. The starlings migrate via quantum random dives (QRD), both downward and upward. Equation (7) displays the two quantum possibilities that the starlings in a flock use to toggle between these quantum dives. The downward and upward probability is represented by the variables $|\psi^{Up}(W_j)|\ and\ \left|\psi^{Down}(W_j)\right|$ respectively and calculatedthe Equations (8) and (9). The user sets the variables $\varphi\ and\ \theta$, and the inverse-Gaussian dispersion $|\psi(\delta_2)\rangle$ is generated using Equation (10), where λ and μ are user-set values and y is an arbitrary integer.

$$RQC = \begin{cases} \text{Upward quantum dive} \left|\psi^{Up}(W_j) > \psi^{Down}(W_j)\right| \\ \text{Downward quantum dive} \left|\psi^{Up}(W_j) \leq \psi^{Down}(W_j)\right| \end{cases} \quad (7)$$

$$|\psi^{Up}(W_j)\rangle = f^{j\varphi} cos\theta \times |\psi(\delta_2)\rangle - f^{-j\varphi} sin\theta \times |\psi(\delta_2)\rangle \quad (8)$$

$$|\psi^{Up}(W_j)\rangle = f^{j\varphi} sin\theta \times |\psi(\delta_2)\rangle + f^{-j\varphi} cos\theta \times |\psi(\delta_2)\rangle \quad (9)$$

$$|\psi(\delta_2)\rangle = \sqrt{\frac{\lambda}{2 \times \pi \times z^3} \times f\left[\frac{\lambda(z-\mu)^2}{2 \times \mu^2 \times z}\right]} \quad (10)$$

The quantum dives, both downward and upward are calculated with Equations (11) and (12), respectively, wherein $|\psi(Q_C)\rangle$ is chosen from set Q, $|\psi(W_j)\rangle$ is the location of starling t_j in the current each iteration, the location of $|\psi(W_q)\rangle$ is chosen at arbitrarily among flocks allocated for diving strategy and the greatest starlings set and individuals T are chosen at arbitrary. $|(\delta_1)\rangle$are an arbitrary location chosen from the best starlings set from the first iteration and the starling population T.

$$|\psi \quad (s+1, W_j)\rangle = |\psi \quad (Q_C)\rangle - |\psi^{Down}(W_j)\rangle \times |\psi \quad (W_j)\rangle - |\psi \quad (W_q)\rangle R_r(s) = \frac{\sum_{j=1}^{l} \frac{1}{m} \sum_{i=1}^{m} te_{ji}(s)}{\frac{1}{m} \sum_{i=1}^{m} te_{ji}(s)} \quad (11)$$

$$|\psi(s+1, W_j)\rangle = |\psi(Q_C)\rangle + |\psi^{Up}(W_j)\rangle \times \left(|\psi(W_j)\rangle - |\psi(W_i)\rangle + \psi(\delta_1)\rangle\right) \quad (12)$$

Swirling Search Strategy: When the level of quality in a flock is greater than the average quality of all flocks $\left(R_r(s) > \mu_R(s)\right)$, starlings inside the flock will take advantage of the search difficulty by employing the swirling search method. Equation (13), which describes the whirling search tactics, states that $W_j\ (s+1)$ is the starling t_j's next position at repetition s, and the location $W_{QX}\ (s)$ was selected at random from set Q of flocks that qualify for the swirling search strategy, and $W_M\ (s)$ is arbitrarily selected from all flocks that wish to use the swirling search strategy. Equation (14) is used to determine$D_j\ (s)$, the cohesion operator. $\xi\ (s)$ is an arbitrary number between 0 and 1.

$$W_j(s+1) = W_j(s) \times D_j(s) \times \left(W_{QX}(s) - W_M(s)\right) \quad (13)$$

$$D_j(s) = \cos(\xi(s)) \quad (14)$$

YOLO-V7: The YOLO method, the most common example of a single-stage detection technique, depends on deep neural networks for identifying objects and molecule. To accomplish end-to-end target recognition, it employs the same CNN model. The entire picture is fed into a network structure and the limiting box's position and associated category are regressed in its result layer. A fair compromise between accuracy and operation speed is offered by the YOLO-V7 system, which is a continual development over the YOLO series. The YOLO-V7 network is divided into four basic modules: input, backbone, head, and prediction. It uses methods like re-parameterized convolution, model expansion for concatenation-based models, expanded efficiency layer aggregating networks (E-ELAN), and others. **Figure 2**

displays the YOLO-V7 algorithm structure.

Within the YOLO-V7 backbone system, computer block E-ELAN can facilitate the learning of more varied properties by various groups of computing blocks. In large-scale ELANs, the network achieves equilibrium, irrespective of gradient direction, path length, or total number of blocks. If the blocks are stacked indefinitely, such states of equilibrium may be eliminated and the use of the main settings minimized. The E-ELAN method employs expansion, random scrambling, and merging cardinality to improve network training ability while preserving the original gradients route, as well as to direct the various computationally block groups to acquire varied characteristics of molecule. The basic goal of scaling the model is to alter the model's unique features and build model of various sizes to satisfy the demands of different inferences speeds. For a cascade-based approach, the remaining portion of the layer of transport is scaled with the equivalent width and the level in the computation block has to be changed. When a computed block's depths factor is scaled, the change in the block's outputs channel is determined, and the change of layer is updated accordingly. With advice from the instruction head's prediction outcomes, RepConv absent constant interaction is used to remodel the reparametrized convolution's structure and suggests generating coarse to suitable hierarchy labels that aid in the guidance head's learning.

Adaptive YOLO-V7: There are three sizes for the head in the original YOLO-V7 algorithm: large, medium, and small. The investigation discovered that hidden targets raised the error rate during the extraction of features based on the real distributions and sample circumstances of T. Additionally, the object of extraction was insufficient due to disturbance and decreased precision in identifying targets at small distances. As a result, this study suggested extending the layer to the original, dropping generated feature map, inserting an object recognition layer, and further influencing the data flow. **Figure 3** depicts how the updated map of features made easier to provide the target's feature data and meet the goal of enhancing the accuracy of detection.

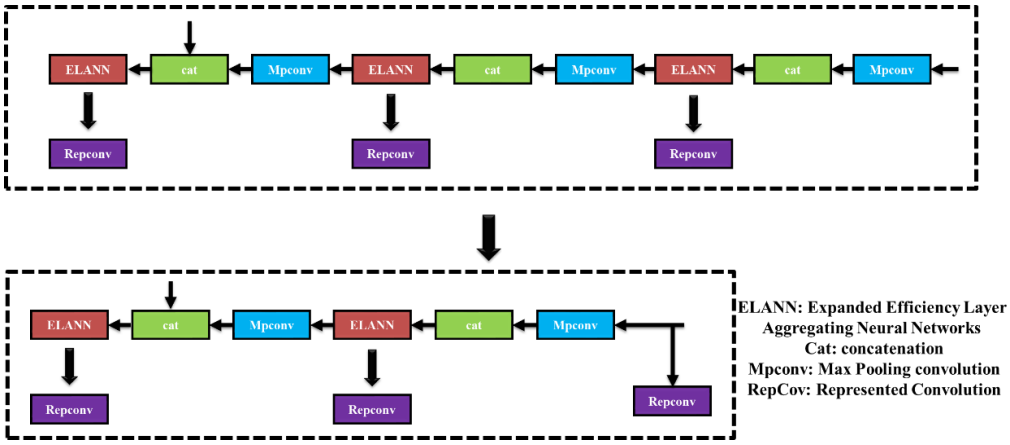

Figure 3. Enhancements to the detecting head.

SM-AYOLOv7: The improved SM-AYOLOv7, enhances the traditional YOLOv7 framework by integrating adaptive mechanisms tailored for detecting complex flocking behaviors in starlings. This algorithm employs a refined feature

extraction process that focuses on the unique motion patterns and formations characteristic of murmurations, allowing for improved accuracy in identifying individual birds within densely packed groups. By leveraging advanced techniques such as attention mechanisms and multi-scale feature aggregation, SM-AYOLOv7 optimizes the model's performance, enabling it to effectively handle variations in lighting, density, and occlusion. The goal of outdoor rural planning is to bring harmony between the natural constituents with human needs, through the integration of biodiversity, sustainable solutions, and cultural identity into the plans. This complex assignment in the identification of core indicators and establishment of biomechanics requires the most perfect and expedient instruments for data analysis of various rural regions.SM-AYOLOv7 algorithm which relies on the remote sensing image technology integrated with collected data from the UAVs will be used to develop a training model which could do landscape with precision. For satisfactory space-of-place rendering, a 3D GIS virtual imaging design will be employed which depicts the rural landscape with an acceptable level of accuracy. The new SM-AYOLOv7 stands out with its inspiration from born-starring-like flocking behavior. Consequently, this approach continues making improvements in the network parameters to further improve YOLOv7's ability to detect objects, which is the case with accuracy and efficiency. The illustrious intelligence system illustrates the hypothetically adaptive and collective behaviors of starling flocks helping the model to accomplish a precise classification of human environments and rural buildings. As a result, it significantly boosts detection speed and precision, making it well-suited for real-time applications in wildlife monitoring and research. The technique for SM-AYOLOv7 is shown in Algorithm 1.

Algorithm 1 SM-AYOLOv7

Initialize parameters:
- Define starlings' group T (size M), set search space dimensionality C, and limits W^K (lower) and W^V (upper).

2. Initialize starling positions and fitness scores:
- For each starling t_j in T:
- Generate position $W_j(s)$ and calculate fitness score $E_j(s)$.

3. Perform iterations until convergence:

a. Separate search strategies:
- Calculate segregated set size O_{sep} and select starlings from T to form segregated sets
- Modify selected starlings and update starling positions.

b. Allocate remaining starlings for diving or swirling search strategies:
- Form non-empty flocks and evaluate effectiveness.
- Assign search strategies based on flock conditions.

c. Diving search strategy:
- Use quantum random dives (QRD) for selected flocks and update the starling positions based on probabilities.

d. Swirling search strategy:
- Implement swirling search method for eligible flocks and update the starling positions.

4. Repeat steps 3 until convergence criteria are met.

5. Output the optimized positions of starlings.

5. Result and analysis

On a Windows 11 OS, we used the Python programming language (version 3.10) to implement our technique. An Intel Core i7 CPU drove the computational environment, which was accompanied by a high-performance IRIS graphics card to ensure that complicated machine-learning tasks were completed efficiently. The

efficacy of the proposed technique (SM-AYOLOv7) was assessed using a range of criteria, such as recall, f1-score, IoU, and precision. The results were compared to those of other methods, such as ((multiple attention gate modules and a context collaboration network) AGSCNet [26], (HighResolution Net) HRNet [27], and (Multi-Attention-Detail U-shaped Network) MAD-UNet) [28].

The adopted approach to organize planning for the dislocation and aggregation of mountain villages was represented by a model of their structural classification. In all unincorporated villages of the given region, village architectural buildings were classified into four series with distinguished features, mentioned and as shown in **Table 1** and **Figure 4**.

Table 1. Classification of building structures.

Category	Characteristics of exterior materials and exterior	Building stories (height) and types of structure
Category A	masonry or reinforced concrete construction	Consists of buildings with 3 stories or more, and those with brick or reinforced concrete construction below three levels
Category B	brick, mud, and wood were used in its construction.	Typically found in buildings spanning 2 to 3 stories, featuring brick or a combination of materials for construction
Category C	Made of mud and wood devoid of embellishment	Generally found in 1 or 2-story buildings with simplistic or aged structural designs
Category D	Comprising mud and wood exhibiting surface deterioration	Typically, single-story structures with extensively damaged walls, beams, and roofs

Figure 4. Categorization of constructionstructures.

Figure 5 demonstrated that the diffusion and the number of buildings would affect the image perception results greatly. Researchers used the imaging data to identify the buildings that were scattered and those were densely clustered. The ones with fewer buildings do a better job in terms of recognition the ones with densely clustered buildings may simply obstruct the recognition process through biomechanics. **Table 2** shows the process of Overall comparison of detection models.

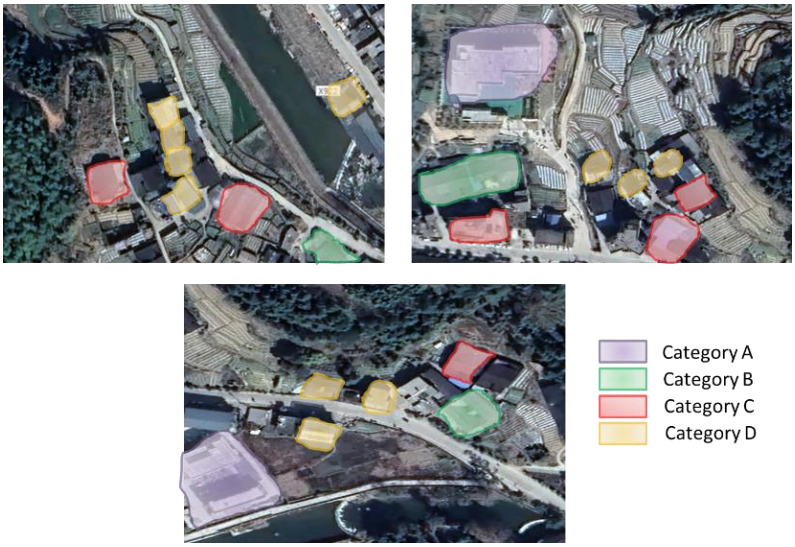

Figure 5. Consequences of recognition.

Table 2. Performance comparison of object detection models.

Methods	Precision (%)	Recall (%)	F1-score (%)	IoU (%)
AGSCNet	86.31	77.16	81.49	68.76
HRNet	77.75	67.03	63.23	56.24
MAD-UNet	88.39	86.19	87.28	77.43
SM-AYOLOv7 [Proposed]	91.72	92.34	93.64	90.23

5.1. Precision

The purpose of the study was to examine the precision of the SM-AYOLOv7 algorithm for rural landscape classification. **Figure 6** proved stronger in recognizing and category buildings and environments at remote locations, which was due to the eagle-spotted search strategy. The suggested method, SM-AYOLOv7, obtained a precision of 91.72%, while the results of AGSCNet, HRNet, and MAD-UNet were only 86.31%, 77.75%, and 88.39%, respectively.

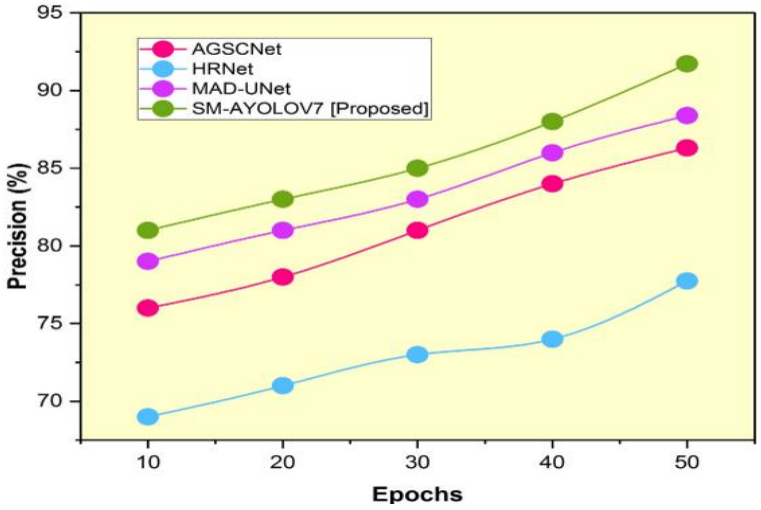

Figure 6. Comparison of precision.

5.2. Recall

Study assessed the SM-AYOLOv7 algorithm for rural landscape classification, which was compared with the traditional methods to find the recall. **Figure 7** values representation significantly, notably for identifying structures and environments in the rural areas. The suggested method, SM-AYOLOv7, obtains a recall of 92.34%, while the results of AGSCNet, HRNet, and MAD-UNet were only 77.16%, 67.03%, and 86.19%, respectively.

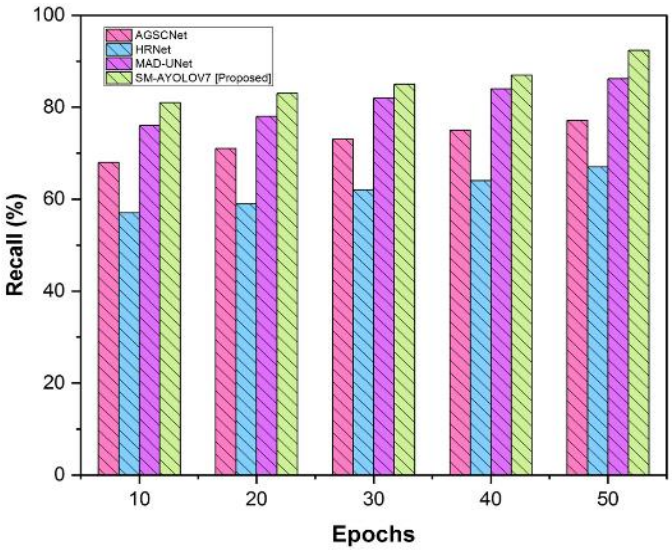

Figure 7. Comparison of recall.

5.3. F1 score

Research evaluated the SM-AYOLOv7 algorithm's F1 score objective measurements. **Figure 8** enhanced performances is attributed to the innovation of the constellation-swarming algorithm that enables the robot to have an increased number of search tactics with inferring the precision and recall and thereof higher F1 values. The suggested method, SM-AYOLOv7, obtains anf1 score of 93.64%, while the results of AGSCNet, HRNet, and MAD-UNetwere only 81.49%, 63.23%, and 87.28%, respectively.

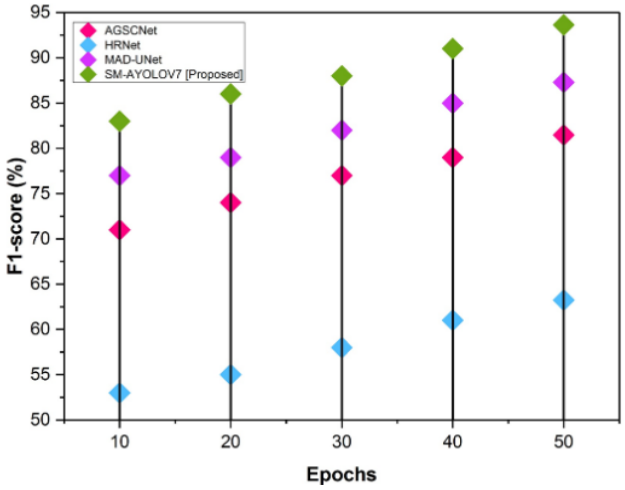

Figure 8. Comparison of F1 score.

5.4. IoU

Study assessed the IoU performance of the SM-AYOLOv7 algorithm vs the conventional methodologies for the classification of rural landscapes. **Figure 9** obtained SM-AYOLOv7 always achieved the highest IoU scores, which means more successful than other approaches in localizing the features of the rural landscape. The suggested method, SM-AYOLOv7, obtains an IoU of 90.23%, while the results of AGSCNet, HRNet, and MAD-UNetwere 68.76%, 56.24%, and 77.43%, respectively.

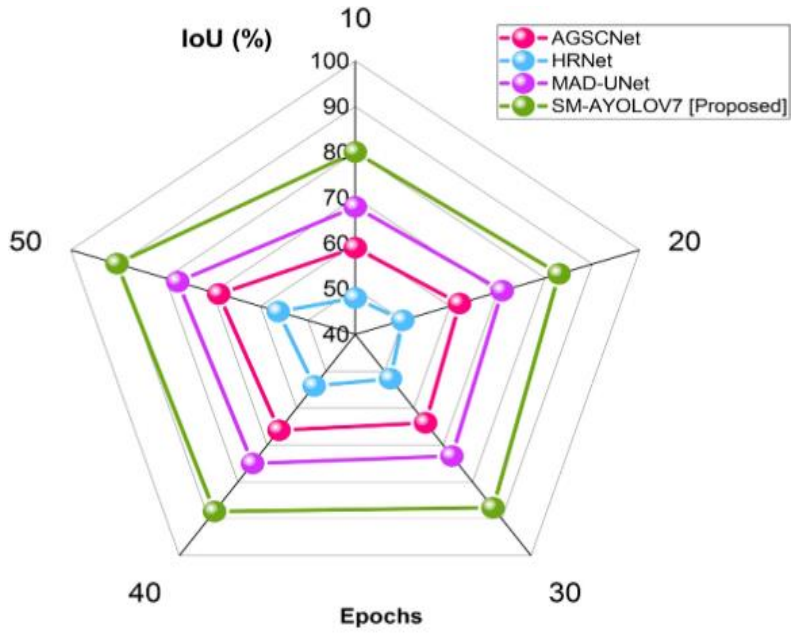

Figure 9. Comparison of IoU.

6. Conclusion

This research exhibits a new method of designing rural landscapes with the use of remote sensing imagery and the SM-AYOLOv7 algorithm. Through the integration of 3D GIS virtual imaging design models and the application of SM optimization, our proposed model reveals a heightened precision and efficiency in the rural building and environment identification process informed by biomechanics at the molecular level. The outcomes of our analysis prove that our method is better than the conventional ones, thus increasing the chances of more exact and flexible rural landscape design practices. This research, becomes a stepping stone in the development of the field of landscape design through the use of the latest technology to produce, in most cases, sustainable environments will be great benefit to both ecosystems and communities. This research is based on the remote sensing imagery, which may be weakened by factors such as the image resolution and cloud cover, thus affecting the classification results accuracy. Future research could delve into the area of the combining of real-time data streams and advanced machine learning techniques, thus making the rural landscape design simulations more accurate and adaptable, with a focus on biomechanics to better understand how physical forces interact with the environment and influence design outcomes.

Author contributions: Conceptualization, KX and YX; methodology, KX; software, KX; validation, KX and YX; formal analysis, KX; investigation, KX; resources, KX; data curation, KX; writing—original draft preparation, KX; writing—review and editing, KX; visualization, KX; supervision, KX; project administration, KX; funding acquisition, YX. All authors have read and agreed to the published version of the manuscript.

Funding: This research was funded by [2022 Anhui Provincial Research Preparation Program Project-Key Project Name: Beautiful Rural Living Environment Planning and Design Paradigm Project Name and Practice-Taking Hongguang Village, Laoqiao Town, Zhengpugang New District as an Example] grant number [2022AH050304]. This research was also funded by [Key Laboratory of Multidisciplinary Management and Control of Complex Systems of Anhui Higher Education Institute.Project Name: The Open Fund of Key Laboratory of Anhui Higher Education Institutes (Anhui University of Technology)] grant number [CS2022-02].

Ethical approval: Not applicable.

Conflict of interest: The authors declare no conflict of interest.

References

1. Vucetich, J.A., Macdonald, E.A., Burnham, D., Bruskotter, J.T., Johnson, D.D., & Macdonald, D.W. . (2021). Finding purpose in the conservation of biodiversity by the commingling of science and ethics. Animals, 11(3), 837.
2. Lin, Z.H.E.N., Zengrang, X.U., &Wuxue, C.H.E.N.G. . (2022). Ecological protection and livelihood improvement in ecologically vulnerable regions. Journal of Resources and Ecology, 13(5), 759-762.
3. Thorn, J.P., Thornton, T.F., Helfgott, A., & Willis, K.J. . (2020). Indigenous uses of wild and tended plant biodiversity maintain ecosystem services in agricultural landscapes of the Terai Plains of Nepal. Journal of ethnobiology and ethnomedicine, 16, 1-25.
4. Hu, Y., Tian, Q., Zhang, J., Benoy, G., Badreldin, N., Xing, Z., Luo, Z., & Zhang, F. . (2022). Effectiveness of Chinese pine (Pinustabulaeformis) plantation at reducing runoff and erosion rates in Anjiagou Watershed in the Semi-arid Region of Gansu, China. Plos one, 17(7), e0271200.
5. Kim, H.S., Lee, S.H., Jo, H.Y., Finneran, K.T., & Kwon, M.J. . (2021). Diversity and composition of soil Acidobacteria and Proteobacteria communities as a bacterial indicator of past land-use change from forest to farmland. Science of the Total Environment, 797, 148944.
6. Irvine, K., Dickens, C., Castello, L., Bredin, I., & Finlayson, C.M. . (2022). Vegetated wetlands: from ecology to conservation management. In Fundamentals of Tropical Freshwater Wetlands (pp. 589-639). Elsevier.
7. Moses, T.C. . (2021). Improving staff retention in adolescent psychiatric residential treatment facilities (Doctoral dissertation, Walden University).
8. Tanguay, L. . (2021). How Preserving Biodiversity Mitigates the Impacts of Small-scale Land Grab on Livelihoods and Agricultural Production in Central Java. Kasarinlan: Philippine Journal of Third World Studies.
9. Yang, Z., Yu, X., Dedman, S., Rosso, M., Zhu, J., Yang, J., Xia, Y., Tian, Y., Zhang, G., & Wang, J. . (2022). UAV remote sensing applications in marine monitoring: Knowledge visualization and review. Science of The Total Environment, 838, 155939.
10. Roslim, M.H.M., Juraimi, A.S., Che'Ya, N.N., Sulaiman, N., Manaf, M.N.H.A., Ramli, Z., &Motmainna, M. . (2021). Using remote sensing and an unmanned aerial system for weed management in crops: A review. Agronomy, 11(9), 1809.
11. Shan, P., & Sun, W. . (2021). Auxiliary use and detail optimization of computer VR technology in landscape design. Arabian Journal of Geosciences, 14(9), 798.
12. Liu, X. . (2020). Three-dimensional visualized urban landscape planning and design based on virtual reality technology. IEEE access, 8, 149510-149521.

13. Shan, P., & Sun, W. . (2021). Research on 3D urban landscape design and evaluation based on geographic information system. Environmental Earth Sciences, 80(17), 597.
14. Li, R., & Xu, D. . (2020). Distribution of landscape architecture based on 3D images and virtual reality rationality study. IEEE access, 8, 140161-140170.
15. Deneu, B., Joly, A., Bonnet, P., Servajean, M., & Munoz, F. . (2022). Very high resolution species distribution modeling based on remote sensing imagery: how to capture fine-grained and large-scale vegetation ecology with convolutional neural networks?. Frontiers in plant science, 13, 839279.
16. Wang, R., Gao, W., Zhou, N., Kammen, D.M., & Peng, W. . (2021). Urban structure and its implication of heat stress by using remote sensing and simulation tool. Sustainable Cities and Society, 65, 102632.
17. Luo, J. . (2021). Online design of green urban garden landscape based on machine learning and computer simulation technology. Environmental Technology & Innovation, 24, 101819.
18. Zhai, Y., & Li, W. . (2022). Study on the Construction of Landscape Architecture in Residential District Based on Urban Greening Remote Sensing. Journal of Sensors.
19. Peng, L. . (2021). Intelligent landscape design and land planning based on neural network and wireless sensor network. Journal of Intelligent & Fuzzy Systems, 40(2), 2055-2067.
20. Li, H., Fang, C., Xia, Y., Liu, Z., & Wang, W. . (2022). Multi-scenario simulation of production-living-ecological space in the Poyang Lake area based on remote sensing and RF-Markov-FLUS model. Remote Sensing, 14(12), 2830.
21. Huang, Y., Peng, H., Sofi, M., Zhou, Z., Xing, T., Ma, G., & Zhong, A. . (2022). The city management based on smart information system using digital technologies in China. IET Smart Cities, 4(3), 160-174.
22. Aslam, R.W., Shu, H., Naz, I., Quddoos, A., Yaseen, A., Gulshad, K., &Alarifi, S.S. . (2024). Machine Learning-Based Wetland Vulnerability Assessment in the Sindh Province Ramsar Site Using Remote Sensing Data. Remote Sensing, 16(5), 928.
23. Feng, Q., Niu, B., Chen, B., Ren, Y., Zhu, D., Yang, J., Liu, J., Ou, C., & Li, B. . (2021). Mapping of plastic greenhouses and mulching films from very high resolution remote sensing imagery based on a dilated and non-local convolutional neural network. International Journal of Applied Earth Observation and Geoinformation, 102, 102441.
24. Yi, J.J., & Xiao, Y.X. . (2021). Spatial-temporal evolution of complex urban landscape pattern based on remote sensing technology. International Journal of Environmental Technology and Management, 24(1-2), 62-76.
25. Al-Hameedi, W.M.M., Chen, J., Faichia, C., Al-Shaibah, B., Nath, B., Kafy, A.A., Hu, G., & Al-Aizari, A. . (2021). Remote sensing-based urban sprawl modeling using multilayer perceptron neural network markov chain in Baghdad, Iraq. Remote Sensing, 13(20), 4034.
26. Yu, M., Zhou, F., Xu, H., & Xu, S. . (2023). Advancing Rural Building Extraction via Diverse Dataset Construction and Model Innovation with Attention and Context Learning. Applied Sciences, 13(24), 13149.
27. Sun, K., Xiao, B., Liu, D., & Wang, J. . (2019). Deep high-resolution representation learning for human pose estimation. In Proceedings of the IEEE/CVF conference on computer vision and pattern recognition (pp. 5693-5703).
28. Xue, H., Liu, K., Wang, Y., Chen, Y., Huang, C., Wang, P., & Li, L. . (2024). MAD-UNet: A Multi-Region UAV Remote Sensing Network for Rural Building Extraction. Sensors, 24(8), 2393.